Global diagnostics of the operational AVHRR SST and aerosol retrievals from NOAA-16 and -17

Alexander Ignatov*[a], John Sapper[b], William Pichel[a], Eileen Maturi[a], Andy Harris[c], Alan E. Strong[a], Eric Bayler[a], Istvan Laszlo[a], Nicholas Nalli[d], Xiaofeng Li[e]

[a]NOAA/NESDIS, Office of Research and Applications, 5200 Auth Road, Camp Springs MD 20746
[b]NOAA/NESDIS, Office of Satellite Data Processing and Distribution, FB4, Suitland, MD 20746
[c]CICS, University of Maryland, College Park, MD 20742
[d]QSS Group Inc., Lanham, MD 20706
[e]DSTI Inc., Camp Springs, MD 20746

ABSTRACT

Under cloud-free conditions during the daytime, global synergistic retrievals of sea surface temperature (SST) and aerosol optical depths (AOD, or) are made from the AVHRR instruments flown onboard polar-orbiting sun-synchronous NOAA-16 (equator crossing time, EXT~1400) and -17 (EXT~1000) satellites. Validation against buoys and sun-photometers is customarily considered the ultimate check of the quality and accuracy of SST and AOD retrievals. However, ground-truth data are not available globally and their quality is non-uniform. Moreover, the remotely-sensed parameters may not be fully comparable with their counterparts measured from the surface (e.g. skin vs. bulk SST), and the current procedures to merge data in space and time are not fully objective and may themselves introduce additional errors. In this paper, we propose to supplement the traditional validation with another global diagnostic system. The proposed Quality Control/Assurance (QC/QA) system is based on a comprehensive set of statistical self- and cross-consistency checks. Here, it is illustrated with 8 days of global NOAA-16 and -17 data in December 2003. The AODs and SST anomalies have been first aggregated into 1-day, 1-degree boxes, and their global statistics examined. Analyses are best done in anomalies from the expected state (climatology), which is currently available for the SST but not for the AOD. Histograms of NOAA-16 and -17 SST anomalies are highly correlated (R~0.77), both showing an approximately Gaussian shape, with a mean of ~+0.3K and RMS~1K. AODs also show much similarity but reveal significant cross-platform biases. The magnitudes and even the signs of these biases are band-specific, suggesting that they are due to calibration differences between the two AVHRRs flown on the two platforms. Recall that the AVHRR solar reflectance bands used for aerosol retrievals lack on-board calibration, and therefore may be subject to large calibration errors.

Keywords: NOAA, AVHRR, aerosol optical depth, sea surface temperature, consistency checks.

1. INTRODUCTION

Advanced Very High Resolution Radiometers, AVHRR, have been flown onboard NOAA satellites since 1978. In 1981, NESDIS had developed and successfully implemented the global operational multi-channel SST (MCSST) product from AVHRR Earth emission bands (EEB)[1]. The SST (or T_S) equations are applied only to those AVHRR pixels which have been navigated, calibrated, cloud screened and quality controlled. Currently, these pre-processing functions are performed within a complex mainframe-based system called the Main Unit Task (MUT). With the launch of NOAA-11 in 1990, NESDIS launched another operational product from the AVHRR over the global ocean, the aerosol optical depth (AOD or τ)[2]. Data in AVHRR solar reflectance bands (SRB) processed within the same MUT system are utilized for the τ-retrievals. As of today, operational SST and AOD retrievals are made from two platforms, NOAA-16 and -17, using the non-linear SST (NLSST) and the 3rd generation aerosol algorithms[3,4].

Sampling domains for the SST and AOD products differ significantly. Aerosol retrievals are not made during nighttime and in areas contaminated by sun-glint (defined as an area within a 40° glint angle cone around the specular point), and on the solar side of the orbit. For this study, we have chosen to analyze a combined SST/aerosol sample, in which each

*Alex.Ignatov@noaa.gov; phone (301)763-8053 ×190; fax (301)763-8572.

Applications with Weather Satellites II, edited by W. Paul Menzel, Toshiki Iwasaki,
Proceedings of SPIE Vol. 5658 (SPIE, Bellingham, WA, 2005)
0277-786X/05/$15 · doi: 10.1117/12.577952

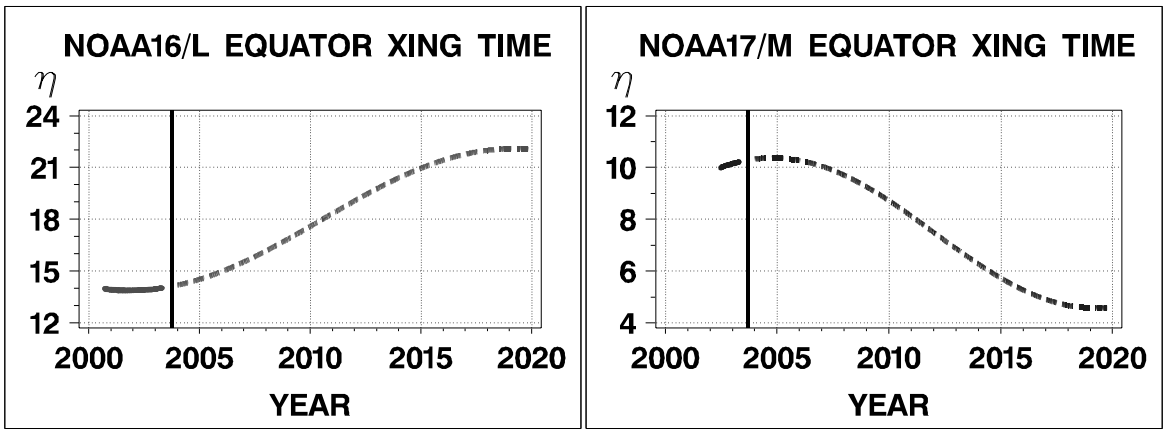

Fig. 1. Local Equator crossing time, η(h), for the NOAA-16 and -17 platforms, and their future projections. For details, see Ref. 5.

observation contains both τ and T_S retrievals. Such data are available from the global Aerosol Observation (AEROBS) files, residing on the NESDIS Central Environmental Monitoring Satellite Computer System (CEMSCS)[4].

Both the SST and AOD global production systems are very complex. As a result, the quality of the final products may depend upon many factors. Performance of the pre-processor (MUT system) is critically important. Also, coefficients of the NLSST equations, which are tuned empirically against buoy measurements early in a platform's lifetime[6], are supposed to hold over time. However, orbital drift of NOAA satellites (Fig. 1) causes systematic changes in the sampled domains of illumination and diurnal cycle. The aerosol algorithm, on the other hand, is not tuned against sun-photometers. Changes here are expected because the SRBs are not calibrated onboard, their calibration drifts in time and is determined vicariously.

Thus it is imperative that both the SST and AOD products are continuously quality controlled/assured in near-real time. Customarily, this is done through validation against ground-based measurements from buoys (for the SST)[6-7] or sun-photometers (for the AOD)[8,9]. Despite greatly increased density of buoys and sun-photometers in recent years, many areas of the globe remain uncovered by ground measurements[10,11]. As a result, the match-up datasets may not be statistically representative of the global satellite retrievals. Additionally, the accuracy of ground-based measurements is non-uniform and not always well documented[6,8-10]. The retrieved parameters may not be fully comparable with their counterparts measured on the surface level. The procedures to merge satellite and surface data in space and time are not fully objective at this time, thus being another potential source of uncertainty in the validation results.

It has been therefore proposed to supplement the customary validation with a number of *global* self- and cross-

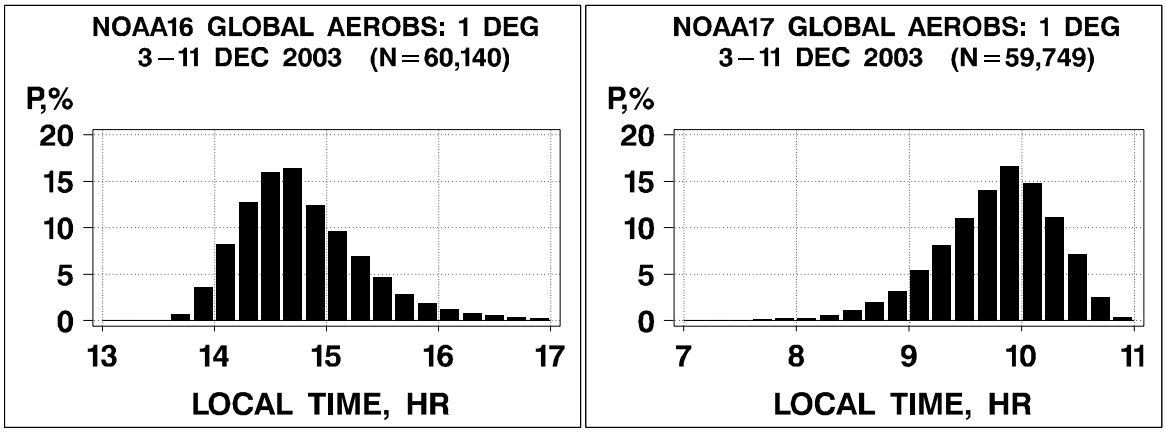

Fig. 2. Histograms of local solar time in AEROBS data from NOAA-16 and -17. Note that solar side of the orbit is excluded from aerosol observations. As a result, both histograms are shifted with respect to the EXT towards lower Sun angle.

consistency checks[12,13]. These checks were originally developed to test global aerosol retrievals. They are based on analyses of global statistical patterns in the retrieved product and their comparisons with those expected from common sense and *a priori* knowledge. Here, they are applied consistently to test the operational NOAAA-16 and -17 SST and AOD global data from 3-11 December 2003. The plan is to test the consistency checks procedures, then combine into a comprehensive QC/QA system, automate for the future continuous use with all AVHRR retrievals, and display the results on the web in near-real time.

2. AEROBS DATA

The AEROBS data reside on the NESDIS CEMSCS as rotating files, one per platform. At each given point in time, each file contains all aerosol and SST retrievals during the last 8 days (approximately representing the full repeat cycle of a NOAA satellite). The files are renewed automatically 4 times a day, around 0100, 0700, 1300, and 1800 EST. For each reported AEROBS pixel (8-km resolution, 2H2 GAC), the following parameters are provided: latitude, longitude, day, local time, sun and view zenith, and relative azimuth angles, reflectances in the SRBs and brightness temperatures in the EEBs, NLSST (T_S), and 3 AODs. In this study, only two AODs are used, τ_1 and τ_2, in AVHRR bands 1 (λ_1=0.63 μm) and 2 (λ_1=0.63 μm), respectively. On NOAA-16, band 3A was discontinued in May 2003 and thus τ_3 is not available in Dec 2003. All SST analyses below are done in anomalies from Bauer-Robinson climatological SST[14], which is also reported on AEROBS. No climate AODs are available at this time.

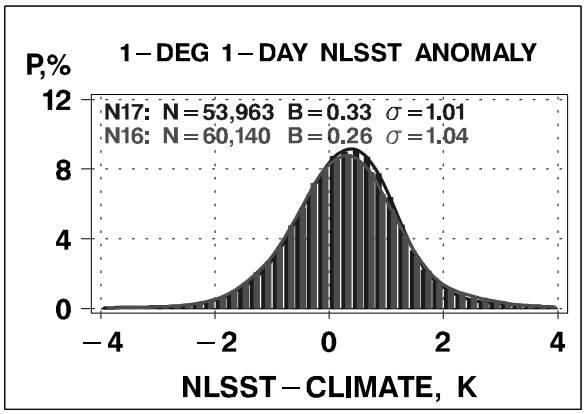

Fig. 3. Global histograms of SST anomalies (NLSST minus Bauer-Robinson[14] climate SST) from NOAA-16 and -17.

For the analyses below, the 8-km AEROBS data from 3-11 December 2003 have been first averaged into 1-day×(1°)^2 space-time boxes, resulting in N=62,197 and 56,054 grids for NOAA-16 and -17, respectively. These data are used in the aerosol analyses below. Climatological SSTs are available in only N=60,140 and 53,963 of those grids. These data are used in the SST analyses below. The observed ~10% sampling difference between the platforms may be due to a sampling of different geographical domains or it may be due to a diurnal cycle in the cloud cover. Or, it may result from the fact that calibration of the AVHRR SRBs, used for cloud screening, are offset between the two platforms (see aerosol analyses below). The NOAA-16 and -17 anomalies samples overlap in a sub-sample called *intersection*, in which both NOAA-16 and -17 data are available. There are N=17,032 such 1-day×(1°)^2 grids (~30% of the full

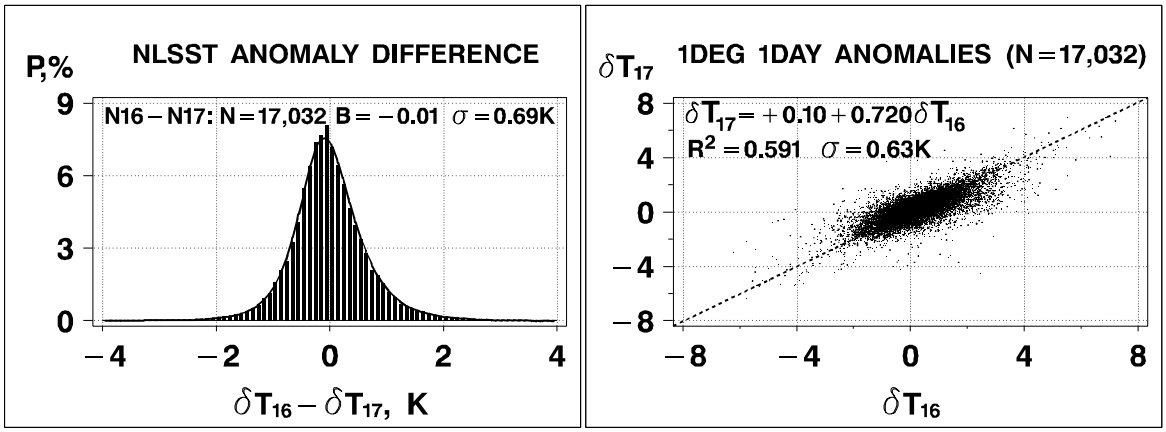

Fig. 4. Left: Histogram of anomalies difference (NOAA-16 minus NOAA-17). The two platforms show close agreement. Right: scattergram of the anomalies (NOAA-17 versus NOAA-16). Larger variability in the afternoon NOAA-16 anomalies compared to the morning NOAA-17 is expected, due to diurnal cycle of SST. Note that both panels are derived from the *intersection* sub-sample in December 2003, which is ~30% of either full sample.

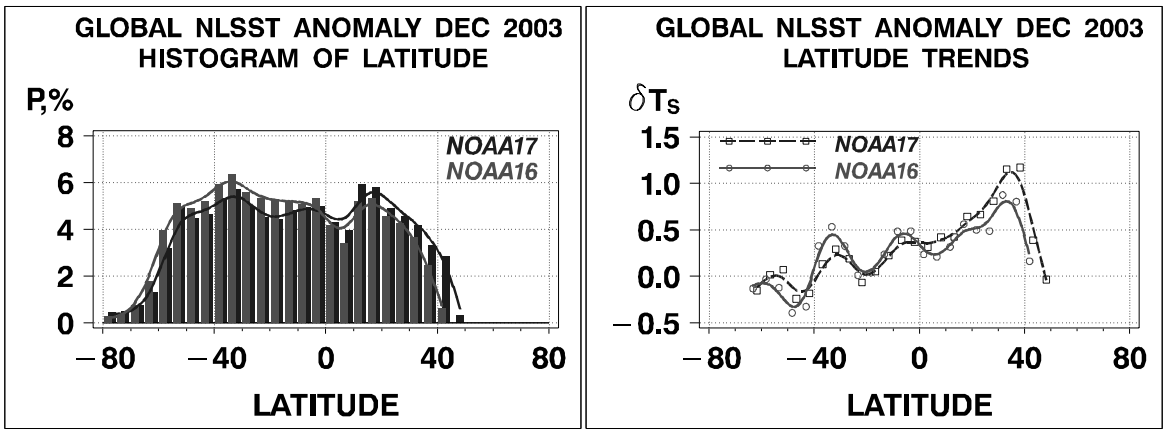

Fig. 5 Zonal densities and trends in SST anomalies derived from the global NOAA-16 and -17 $(1°)^2$-data in December 2003.

samples). In N=43,108 grids, NOAA-16 SST anomalies are available but NOAA-17 are not, and in N=36,931 grids, NOAA-17 anomalies are available but NOAA-16 are not.

In cross-platform comparisons below, one should keep in mind the time difference between the two platforms. NOAA-17 is a morning platform with a nominal equator crossing time, EXT~1000, whereas NOAA-16 is an afternoon platform with a nominal EXT~0200 (Fig. 1). Figure 2 shows that the actual local solar time of AEROBS data may be anywhere within a few hours of the EXT, due to the AVHRR cross-scan and orbital inclinations of the platforms. The diurnal variations in the AOD over global ocean are small and should not affect the results of comparisons[15]. The SST, on the other hand, is known to be subject to the diurnal cycle, which may be significant in areas with weak vertical mixing (low wind speed and high solar insolation).

3. ANALYSES OF SST ANOMALIES

Figure 3 plots global histograms of SST anomalies derived from the two platforms overlaid. They are highly consistent. In particular, their shape is near-symmetric and close to Gaussian. The origin of the global warm bias of +0.30±0.04K is not fully clear at this time. [Recall that the NLSSTs were tuned against buoy SSTs, *independently* for NOAA-16 and -17. The Bauer-Robinson[14] climatology was also derived from ground-based data in mid-1970s.]

The global RMS anomalies are consistent from the two platforms, σ_o~1K (superimposed in Fig. 3). Three factors contribute to σ_o: (1) the real deviation of the retrieved SST from the climate SST, σ_S (i.e., the physical anomaly signal to be estimated from satellite data); (2) the noise, σ_N (representing the RMS error in the satellite retrievals); and (3) the

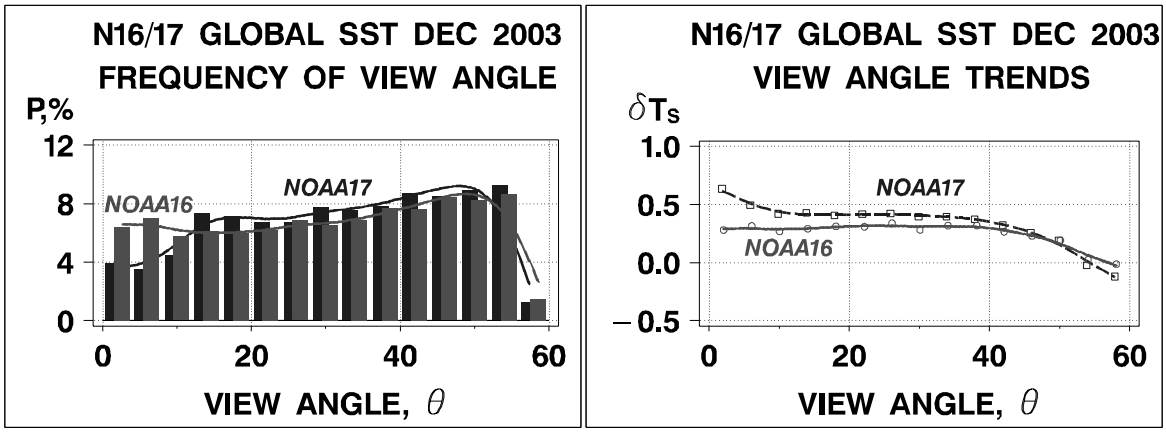

Fig. 6. View angle densities and trends in SST anomalies derived from global NOAA-16 and -17 $(1°)^2$ data in December 2003

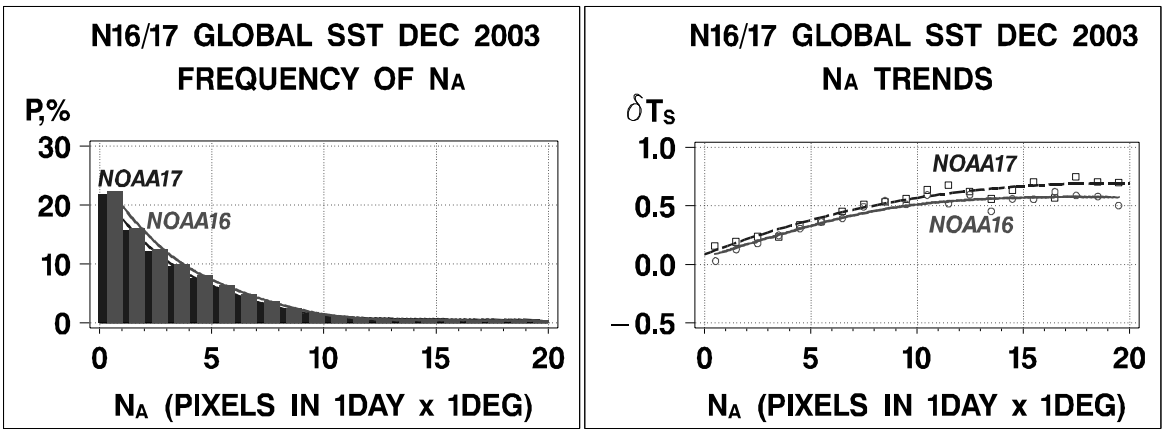

Fig. 7 Densities and trends in SST anomalies vs. population size within $(1°)^2$-boxes (proxy of inverse cloud amount) in Dec 2003.

RMS error in climate SST, σ_C. (Note that the Bauer-Robinson $(1°)^2$ monthly climatology reported on AEROBS is not interpolated in space and time.) Assuming that these components are all independent, one obtains: $\sigma_o^2=\sigma_S^2+\sigma_N^2+\sigma_C^2$.

In order to estimate the noise in satellite retrievals, Fig. 4 plots a histogram of NOAA-16 minus NOAA-17 SST anomaly. The histogram is near-symmetric, close to Gaussian, and shows a negligible cross-platforms bias with an RMS of σ~0.69K. Two factors contribute to the RMS: noise and diurnal SST variability, as the physical anomaly ("signal") and error in climatological SST cancel out in calculating the cross-platform differences. Aside from the global diurnal signal which is not handled properly in the current retrieval system, and assuming that the contributions from the two platforms are comparable and independent, one obtains $\sigma_N\sim\sqrt{\sigma^2/2}\sim0.49$K. (Note that this estimate of σ_N, strictly speaking, is valid for the *intersection* sub-sample only, which is 30% of either full sample and may not be fully representative of the global accuracy of the SST retrievals.)

Note that in addition to being useful to define the SST signal, the SST anomaly lends itself to identifying outliers in the SST retrievals (note that this QC was not attempted in this study). For instance, the minimum anomalies are $\min(\delta T_S)\sim$-9.9K and -7.5K, and the $\max(\delta T_S)\sim$+8.9 and +7.2K from NOAA-16 and -17, respectively. These numbers are outside the $4\sigma_o$ corridor, which is generally considered to be in a valid range[16,17]. Outliers are also seen in the scattergram of NOAA-17 versus NOAA-16 in the second panel of Fig. 4. The correlation between the two anomalies is R~0.77.

Figure 5 shows that the SST anomalies are largely cross-platform consistent in both spatial coverage and reproducible zonal trends. Residual differences may be due to differences in diurnal sampling. In-depth understanding is needed to

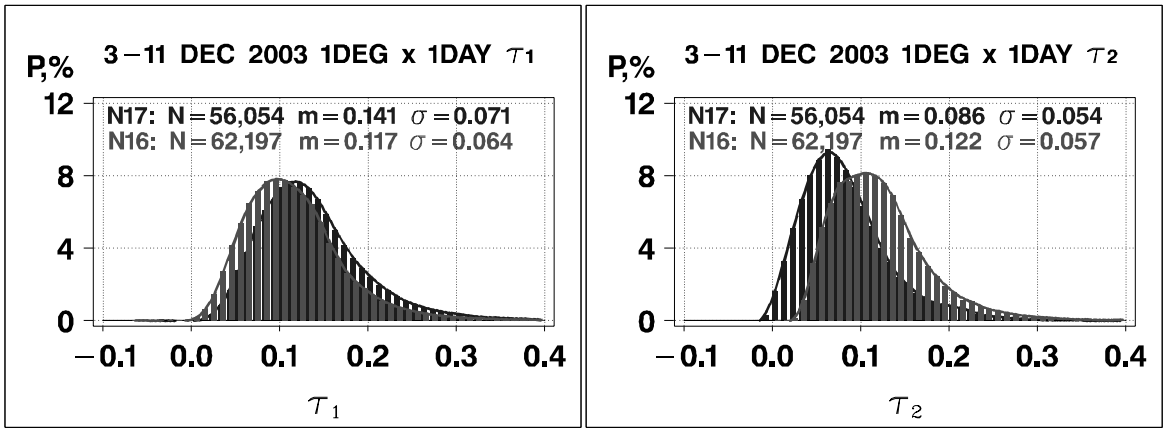

Fig. 8. Global histograms of AODs in AVHRR bands (left) 1 and (right) 2 from NOAA-16 and -17 in December 2003.

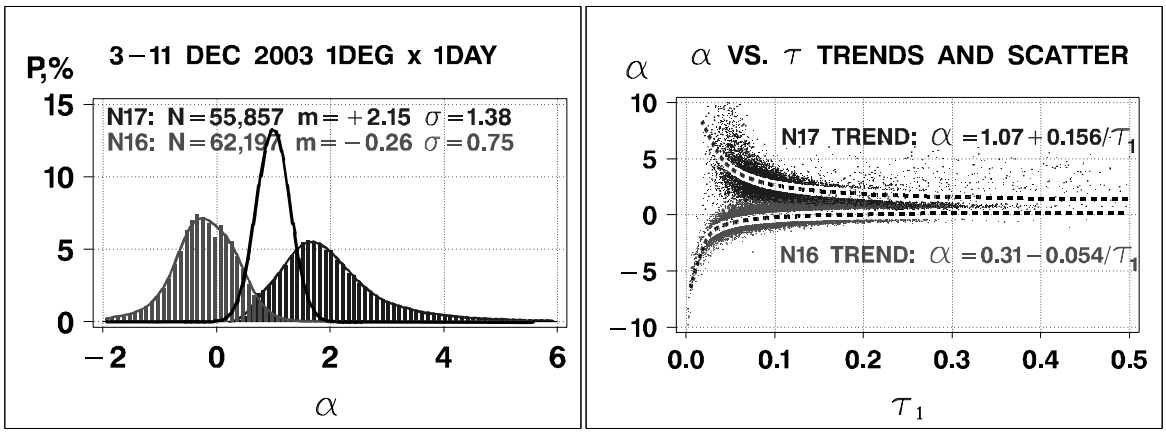

Fig. 9 Left: Histograms of the Angstrom exponent $\alpha=-\ln(\tau_1/\tau_2)/\ln(\lambda_1/\lambda_2)$. Overlaid (in black solid line) is the expected position of α histogram. Right: trends "α vs. τ ". Increasing trends and scatter at low τ are indicative of systematic and random errors in α.

improve the performance of each SST product, and combine the two platform SSTs into a blended product.

Figure 6 plots view angle (θ) densities and trends in the retrievals. The $\delta T_S(\theta)$ are exemplarily flat in the range from θ=0-40°, with the exception of a small-scale near-nadir anomaly in the NOAA-17 data, whose nature is unclear. However, the most prominent feature of Fig.6, a progressively cold bias in δT_S at θ>40°, is clearly seen in the data of both platforms. Recall that the view angle correction in the NLSST algorithm is done empirically[3].

Figure 7 shows the average SST anomaly, δT_S, as a function of number of AEROBS pixels in $(1°)^2$-box, N_A (which is expected to be inversely proportional to the average ambient cloud amount). There is a progressively cold bias at $N_A<10$ (note that the vast majority of $(1°)^2$-boxes belong in this domain). It may be due to the suppressed warming of the surface under cloudy conditions during the daytime. Or, it may be caused by residual cloud in the AVHRR field-of-view. The $\delta T_S(N_A)$ trend flattens out at higher $N_A\geq10$, but there are very few data in this retrieval domain. Qualitatively similar trends have been observed in the earlier SST products[18]. The magnitude of the artifacts has been substantially reduced in the newer products. Note that the sampling bias may also affect the zonal analyses, which show that data density becomes sparser towards high latitudes.

4. ANALYSES OF AEROSOL RETRIEVALS

Figure 8 plots global histograms of AODs in AVHRR bands 1 and 2. Their shape is close to lognormal as expected[19-20].

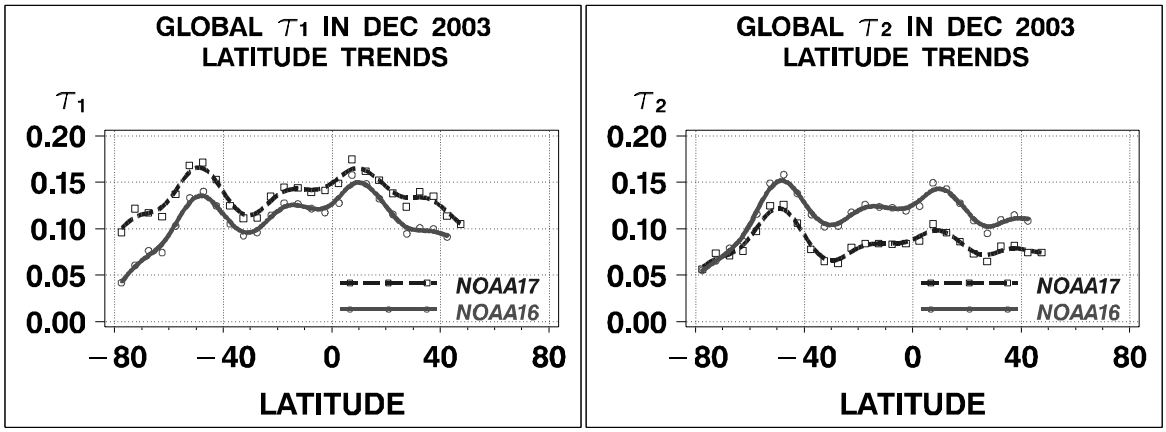

Fig. 10. Zonal trends in τ_1 (left) and τ_2 (right) from NOAA-16 and -17. Trends are qualitatively similar but absolute values of AODs differ, due to the uncertain calibration in AVHRR solar reflectance bands.

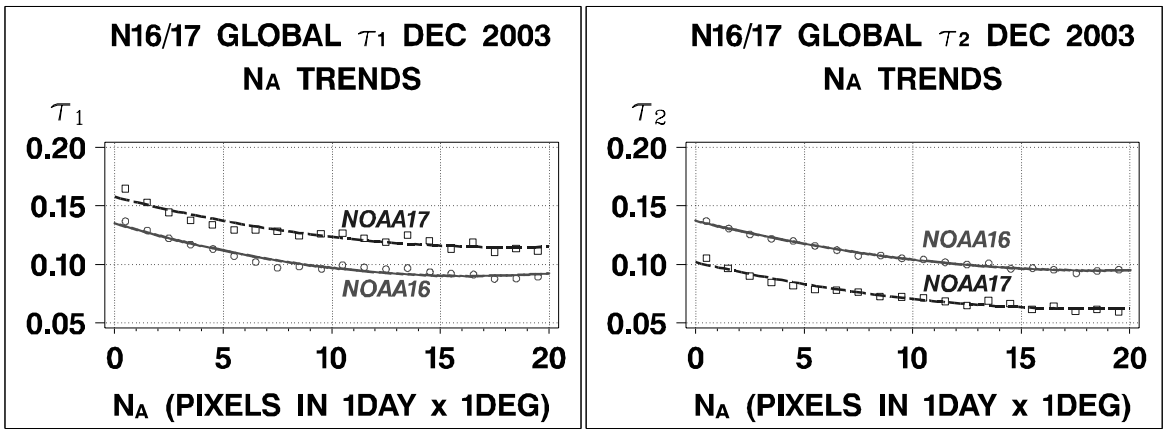

Fig. 11. Trends in AODs vs. population size within $(1°)^2$-boxes (proxy of inverse cloud amount) in Dec 2003. Note increased trends in AODs at low N_A. Cross-platform differences in both bands are caused by AVHRR calibration uncertainties.

Recall that the retrieved τ's are not truncated and, therefore, may go negative due to calibration errors or violation of retrieval assumptions[20]. There are significant cross-platform differences, in both bands. Global average AODs are τ_1=0.117/0.141 and τ_2=0.122/0.086 from NOAA-16/17, respectively. (Compare with τ_1=0.120/0.149 and τ_2=0.102/0.093 in February 2003[4].) The significant cross-platform and temporal τ-differences result from large calibration uncertainties in AVHRR SRBs (which, recall, are lacking onboard calibration, drift with time, and are calibrated vicariously)[4,21].

As a result of erroneous AODs, the Angstrom exponent, derived from the two bands as $\alpha=-\ln(\tau_1/\tau_2)/\ln(\lambda_1/\lambda_2)$, is also highly uncertain. The left panel of Fig. 9 plots global histograms of α from the two platforms. The expected frequency distribution for α is also superimposed in Fig. 9 in a black solid line[13]. Both empirical α's deviate from the expected Gaussian shape and are biased low/high from NOAA-16/17, respectively. The trends "α vs. τ" (shown in the right panel of Fig. 9) are significant in both platforms and opposite, signaling systematic errors in AODs. The Angstrom exponents are progressively affected by systematic τ-errors (trends) and random τ-errors (scatter) towards low τ[4,20,22]. These results confirm previous observations that errors in AVHRR-derived α exceed the range of its natural variability[4]. Fixing the aerosol model at its global average value, while being an important limitation, provides more stability in the retrieved τ than predicting it from a noisy Angstrom exponent.

Zonal τ-trends shown in Fig. 10 are qualitatively reproducible cross-platform in both AVHRR bands. The quantitative differences are deemed to be chiefly due to calibration errors in the two bands. Comparing zonal τ-trends in Fig. 10 with δT_S,-trends in Fig. 5 suggests that the SST anomalies may be (negatively) correlated with AOD. This correlation is

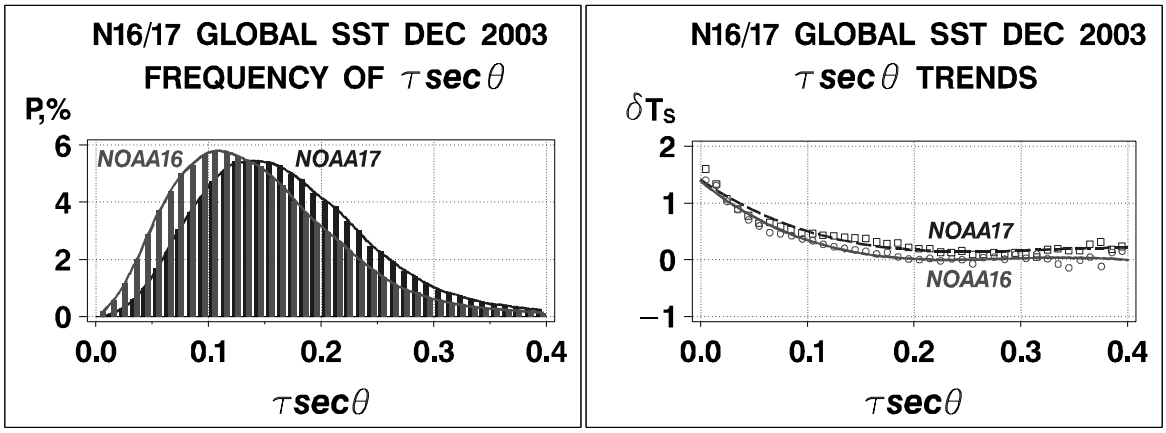

Fig. 12. Frequencies of τsecθ-parameters and trend in SST anomaly. Note a high cross-platform consistency in the $\delta T_S(\tau)$ trends.

explored in section 5.

Figure 11 shows τ-trends as a function of population size within $(1°)^2$-box. All AODs are consistently elevated at low N_A. These aerosol trends have been previously observed in aerosol retrievals from a number of sensors and platforms[4,20,22-25]. They may be due to cloud-aerosol interactions or residual clouds in a sensor field of view. Note that the $\tau(N_A)$ trends are opposite to the $\delta T_S(N_A)$ trends in Fig. 7, possibly suggesting a complex correlation mechanisms between SST on the one hand, and aerosol and residual clouds in a field of view, on the other.

5. SST-AEROSOL CORRELATIONS

Aerosols are known to affect the SST retrievals in the thermal IR[26]. Simple theoretical equations were derived in Ref. 26 to predict the aerosol effect on AVHRR channel 4 and 5 brightness temperatures, T_4 and T_5:

$$\Delta T_4 = A_4 \tau_4 \sec\theta; \qquad \Delta T_5 = A_5 \tau_5 \sec\theta \tag{1}$$

In Eq. (1), θ is the viewing zenith angle, and τ_i are *absorbing* AODs in AVHRR channels i=4 and 5. Note that these thermal IR *absorption* AODs should not be confused with the AODs τ_1 and τ_2, analyzed in section 4, which are mostly *scattering* AODs and are derived in AVHRR bands 1 and 2, separated from bands 4 and 5 in the spectrum by ~10 μm. The proportionality coefficients, A_i, generally depend upon spectral interval, but they are mostly functions of T_S (surface temperature) and T_A (temperature of aerosol layer)[26]:

$$A_i = \left[B(T_S) - B(T_A)\right] \frac{\partial T}{\partial B(T_S)} \approx T_S - T_A \tag{2}$$

The latter approximate equality is not here to be used quantitatively but to demonstrate that the sensitivity of brightness temperature in either AVHRR band to aerosol optical depth (determined by the coefficient A_i) is not a constant and may depend upon e.g. the thermal contrast between the surface and aerosol layer, T_S-T_A.

The aerosol-induced bias in the derived SST is estimated by substituting ΔT_4 and ΔT_5 from Eq. (1) into a SST retrieval equation, such as the MCSST or NLSST. If the aerosol spectral dependence were similar to that of water vapor, then the aerosol effect in the two brightness temperatures would cancel out. However, the spectral dependencies of water vapor and aerosol in the window region are generally opposite: water vapor absorption increases with wavelength whereas the aerosol absorption decreases[28-29]. As a result, the disturbing effect of aerosol is amplified in the MC/NLSST.

There are two ways to deal with aerosol contamination in the SST from AVHRR. One is to utilize the unique information potential of the three AVHRR EEBs and tune the three-channel algorithm to remove effects of both water vapor and aerosol[28-29]. This approach cannot be utilized during daytime however when AVHRR band 3 is contaminated by reflected solar light. The other way is to utilize the visible AODs (τ_1 or τ_2) to predict the τ_4 and τ_5 assuming the that the aerosol spectral dependence (model) non-variable[27,31-31]. Eq.(1) suggest that the SST correction term should be linear with respect to the slant-path AOD in band 1 or 2, $\tau_1\sec\theta$ or $\tau_2\sec\theta$.

Figure 12 shows a correlation of the SST anomaly versus slant-path AOD in AVHRR band 1. Trends from the two platforms are in a remarkable agreement, but they deviate from the expected pattern when the correction looks as a straight line intersecting the origin. Recall that the operational SST equations are empirically tuned to the average atmospheric conditions (i.e. those that include background tropospheric aerosol). As a result, the aerosol-induced bias is expected to be near zero (or ~+0.30K, an average anomaly in our case) at the typical aerosol conditions (represented by a modal value of $\tau_1\sec\theta$~0.13) and not at $\tau_1\sec\theta$~0[27,31]. [Note that the two histograms of $\tau_1\sec\theta$ are shifted with respect to each other, due to the calibration differences discussed in Section 4.] Indeed, the aerosol correction to the SST greatly diminishes in the vicinity of the $\tau_1\sec\theta$-mode. Notre that the dependence δT_S ($\tau_1\sec\theta$) is sharply non-linear. The linearity of the δT_S ($\tau_1\sec\theta$) relationship assumes that all AODs, globally, are located at approximately the same altitude, which may be not the case. The observed non-linearity may thus be related to the fact that different AODs reside on different levels in the atmosphere. Also note that a non-linearity has been observed earlier, but no explanation was offered[27]. Another possible explanation of the observed non-linearity may be due to the fact that the satellite-derived AOD may be subject to residual clouds (cf. trends in Figs. 7 and 11). A ($\tau\sec\theta$) correction is also expected to remove some residual clouds in a satellite field-of-view[27]. Additional research is needed to more fully understand the effect of aerosols on SST, and to correct for them.

6. CONCLUSION

Self- and cross-consistency checks provide a valuable insight into product performance and serve as a useful supplement to the traditional validation against ground-based measurements, which are known to have their own limitations. Analyses of eight days of global SST and aerosol data from NOAA-16 and -17 in this study highlight the following problem areas and potential improvements to the SST and aerosol products from AVHRR.

The SST products are accurate and well reproducible from the two operational platforms. This is expected as SSTs are derived from the well-calibrated AVHRR Earth emission bands, and the coefficients of the NLSST algorithm are tuned empirically against ground-based measurements. There is a positive global bias with respect to the Bauer-Robinson climatology of ~+0.30±0.04K, consistent from both platforms. The nature of this bias is not fully clear at this time, but it may be related to the use of a different base period in the Bauer-Robinson climatology prior to mid-1970s. Random errors in the $(1°)^2$-averaged SST is ~0.5K, globally. More analyses are needed to determine if this error is localized regionally and/or seasonally. It is felt that the SST "noise" can be reduced. One area of improvement is correcting for the effect of the diurnal cycle, and normalizing satellite data to a common observation time. Merging the satellite SSTs with the National Centers for Environmental Prediction (NCEP) forecast is underway to assist with this task. Cold biases in the retrieved SSTs under cloudy conditions, and at high view zenith angles should be understood and corrected for. Development of an accurate aerosol correction to the thermal-IR based SSTs is a long overdue issue.

The AVHRR aerosol product, on the other hand, is derived from the solar reflectance bands, which are not calibrated onboard. Consequently, it is subject to large systematic errors, which, additionally, change in time as the calibration in the AVHRR SRBs degrades. Before an accurate and stable solution is found for the AVHRR calibration, it is recommended to continue using a single-channel methodology for the five Initial Joint POES System (IJPS) platforms (NOAA-N and N´ and METOP-1 to -3) that carry the AVHRR/3 instrument whose reflectance channels are not calibrated onboard. One should keep in mind the qualitative real-time nature of the NESDIS aerosol product and care is advised in their quantitative analyses and use (e.g., for the aerosol correction for SST).

The SST analyses illustrate the critical importance of using climatology in the retrieval process. Ideally, the climatology should be given in terms of (a) multi-year mean (expected state); and (b) multi-year RMS variability. Both parameters should be accurate and be given at high spatial and temporal resolution.

The AVHRR global diagnostic QC/QA system, if developed, will be used for at least 15 more years. NOAA-N will be launched in February 2005 and NOAA-N´ in December 2007, into afternoon orbits. Three European platforms, METOP1-3, carrying the AVHRR/3 sensor will be launched into morning orbits in December 2005, 2010, and 2014, respectively.

ACKNOWLEDGEMNT

Acknowledgement. The SST, aerosol, and cloud products from AVHRR were initiated at NESDIS in the 1980s by P. McClain (retired), N. Rao (deceased), L. Stowe (retired) and C. Walton (retired). The aerosol product has been enhanced and applied to other sensor data (TRMM VIRS, *Terra*/*Aqua* MODIS, and MSG SEVIRI) under the CERES project. The authors are indebted to C. Cao, A. Heidinger, J. Sullivan, and F. Wu (NESDIS) for helpful discussions of the AVHRR radiometric issues. This work was funded under the NASA EOS/CERES (NASA contract L-90987C), the NOAA/NASA/DOD Integrated Program Office, NOAA Ocean Remote Sensing, and the Joint Center for Satellite Data Assimilation (NESDIS) Programs. We thank B. Wileicki (NASA/LaRC), M. Mignogno and T. Schott (NESDIS) and S. Mango (IPO), for their support and encouragement. The views, opinions, and findings contained in this report are those of the authors and should not be construed as an official NOAA or U.S. Government position, policy, or decision.

REFERENCES

1. McClain P., et al, 1985: Comparative performance of AVHRR based multichannel sea surface temperatures, *JGR*, **90**, 11587-11601.
2. Rao N., et al., 1989: Remote sensing of aerosols over oceans using AVHRR data. *Int. J. Remote Sens.*, **10**, 743-749.
3. Walton C., et al., 1998: The development and operational application of non-linear algorithms for the measurement of SST from the NOAA POES. *JGR*, **103**, 27999-28012.

4. Ignatov A., et al, 2004: Operational Aerosol Observations (AEROBS) from AVHRR/3 onboard NOAA-KLM satellites. *JTech.*, **21**, 3-26.
5. Ignatov A., et al, 2004: Equator crossing times for NOAA, ERS, and EOS sun-synchronous satellites. *Int. J. Remote Sensing*, in press.
6. Strong, A., and P.McClain, 1984: Improved ocean surface temperatures from space comparisons with drifting buoys. *BAMS*, **65**, 138-142.
7. Li, X., et al., 2001: Deriving the operational nonlinear multichannel sea surface temperature algorithm coefficients for NOAA-15 AVHRR/3, *Int. J. Remote Sensing*, **22**, *4*, 699–704.
8. Ignatov, A., L.Stowe, S.Sakerin, and G.Korotaev, 1995: Validation of the NOAA/NESDIS satellite aerosol product over the North Atlantic in 1989. *J. Geophys. Res.*, **100**, 5123-5132.
9. Remer, L., et al., 2002: Validation of MODIS aerosol retrievals over ocean. *Geophys. Res. Lett.*, **29**, 8008, doi:10.1029/2001GL013204.
10. Emery, W., et al., 2001: Accuracy of in situ SSTs used to calibrate IR satellite measurements. *J. Geophys. Res,* **106**, 2387-2405.
11. Holben, B., et al., 1998: AERONET – A federated instrument network and data archive for aerosol characterization, Remote Sens. Env., **66**, 1-16.
12. Ignatov, A., and L.Stowe, 2000: Physical Basis, Premises, and Self-Consistency Checks of Aerosol Retrievals from TRMM VIRS. *J. Appl. Meteorol.,* **39**, 2259-2277.
13. Ignatov A., and L.Stowe, 2002b: Aerosol retrievals from individual AVHRR channels: II. Quality control, probability distribution functions, information content, and consistency checks of retrievals. *JAS*, **59**, *3(1)*, 335-362.
14. Robinson M. and A. Bauer, 1985: Description of the Bauer-Robinson numerical atals, ver. VIII, Feb 1985, http://dss.ucar.edu/datasets/ds278.0
15. Kaufman, Y., B.Holben, D.Tanre, I.Slutsker, A.Smirnov, and T.Eck, 200: Will aerosol measurements form Terra and Aqua polar orbiting satellites represent the daily aerosol abundance and properties? *Geophys. Res. Lett.,* **27**, 3861-3864.
16. Ostle, B., and L.Malone, 1988: Statistics in Research, Iowa State University Press/AMES, 664 pp.
17. Bevington, P.R., and D.K.Robinson, 1992: Data Reduction and error Analysis for the Physical Sciences. WCB McGrow Hill, 2nd Ed., 328 pp.
18. Barnett, T., et al., 1979: Climatological usefulness of satellite determined SSTs in the Tropical Pacific. *BAMS*, **60**, 197-205.
19. O'Neill, N., A.Ignatov, B.Holben, and T.Eck, 2000: The log-normal distribution as a reference for reporting aerosol optical depth statistics: Empirical tests using multi-year, multi-site AERONET sun photometer data. *Geophys. Res. Lett.*, **27**, 4778, 3333-3336.
20. Ignatov, A., and L. Stowe, 2002: Aerosol retrievals from individual AVHRR channels. II. Quality control, probability distribution functions and consistency checks of retrievals. *J. Atm. Sci*, **59**, 335-362.
21. Ignatov, A., 2002: Sensitivity and information content of aerosol retrievals from AVHRR: Radiometric factors. *Appl. Opt.,* **41**, 991-1011.
22. Ignatov A. et al., 1998: Sensitivity study of the Ångström exponent derived from AVHRR over oceans. *Adv. Space Res.,* **21**, *3*, 439-442.
23. Ignatov, A., and N.Nalli, 2002: Aerosol retrievals from multi-year multi-satellite AVHRR PATMOS dataset for correcting remotely sensed sea surface temperature. *JTech*, **19**, 1986-2008.
24. Ignatov A., et al, 2004: Two MODIS aerosol products over ocean on the Terra and Aqua CERES SSF datasets. *JAS*, in press
25. Ignatov A., et al, 2004: Aerosol retrievals from TRMM/ VIRS over open oceans. *JAM*, in prep.
26. Strong, A., L.Stowe, and C.Walton, 1983: Using the NOAA7 AVHRR to monitor El Chichon aerosol evolution und subsequent SST anomalies, Proc. 17th Int. Symp. Remote Sensing Env., An Arbor, MI.
27. Griggs M., 1985: A method to correct satellite SST for the effects of atmospheric aerosols, *JGR*, **90**, 12,951-12,959.
28. Walton C., 1985: Satellite measurement of SST in the presence of volcanic aerosols, *JCAM*, **24**, 501-507.
29. Merchant C., et al., 1999: Toward the elimination of bias in satellite SST: I. Theory, modeling, inter-algorithm comparison, *JGR*, **104,** 23,565-23,578.
30. May D., et al., 1992: A correction for Saharan dust effects on satellite SST measurements, *JGR*, **97**, 3611-3619.
31. Nalli, N., and L.Stowe, 2002: Aerosol correction for remotely sensed SSTs from the NOAA AVHRR. *JGR*, **107**, 3172, doi:10.1029/2001JC00162.